

Searching For Crisium Basin Ejecta: Chemistry and Ages of Luna 20 Impact Melts

T. D. Swindle¹, P. D. Spudis^{2,3}, G. J. Taylor⁴, R. L. Korotev⁵,
R. H. Nichols Jr.⁵, and C. T. Olinger⁵

We have performed chemical (INAA) and chronological (⁴⁰Ar-³⁹Ar) analyses of six Luna 20 impact melts, and compared these to the results of Podosek et al. (1973), commonly taken to be representative of the Crisium Basin impact. At least two chemical groups of impact melts are identified. One is interpreted as melts derived from the local crust by craters over the last 3.9 Ga. Another group, which includes one of the samples dated by Podosek et al. (1973), is chemically and chronologically (3.85 ± 0.02 Ga) indistinguishable from Apollo 17 samples interpreted as Serenitatis impact melts, and hence could be melt formed by that event and deposited at the Luna 20 site. One sample (22023,3,F) has a well-defined age of 3.895 ± 0.017 Ga, and is chemically similar to, but distinct from, impact melts from other basins. We tentatively identify this sample, and its chemistry and age, with the Crisium Basin impact. Whether the age of the Crisium impact is given by 22023,3,F, the samples analyzed by Podosek et al. (1973), or neither, it is clear that Crisium impact melt is not abundant in the Luna 20 collection.

INTRODUCTION

The most prominent features on the nearside of the Moon are the large, circular maria. Although the albedo contrast is a result of basaltic lava flows, the extent and location of each mare is determined by that of an ancient crater. Determining the ages, both relative and absolute, of the impacts that formed those craters is important in deciphering the geological history of the Moon. In the present study, we attempt to identify impact melt from the Crisium Basin and to determine the absolute age of the basin.

Crisium appears to be older than Imbrium and younger than Nectaris, whether relative ages are determined by stratigraphy (Wilhelms, 1987), crater counts (Baldwin, 1987b), or rim heights (Baldwin, 1987a). However, its age relative to Serenitatis is less clear. Baldwin (1987a,b) argues that Crisium is younger than Serenitatis, while Wilhelms (1987) suggests that it is older. If any samples date the Crisium impact, they are likely to come from the Luna 20 mission, which landed in highlands south of Mare Crisium, in a region that could be the ejecta blanket from the Crisium impact (see below). The absolute age of Crisium is usually taken to be 3.84 ± 0.04 Ga (Wilhelms, 1987; Deutsch and Stöffler, 1987), based on ⁴⁰Ar-³⁹Ar analyses (Podosek et al., 1973) of two Luna 20 samples, one of them an impact melt, which have identical quoted ages of 3.84 ± 0.04 Ga (recalculated using the decay parameters suggested by Steiger and Jäger, 1977). Cadogan and Turner (1977) also analyzed a Luna 20 impact melt, and obtained an

age of 3.84 ± 0.10 Ga. In his basin chronology, Wilhelms (1987) proposes ages of 3.845 ± 0.030 Ga for Imbrium and 3.87 ± 0.04 Ga for Serenitatis. To be compatible with his proposed relative chronology, the absolute age of Crisium would have to be near the older end of the quoted uncertainties and/or the age of Serenitatis (and perhaps that of Imbrium) would have to be near the younger end of the quoted uncertainties.

As a result of a sample exchange with the Soviet Union, the U.S. obtained a new Luna 20 sample, 22023, in 1987. Upon visual inspection, there were six particles that appeared to be impact melts. This paper reports the results of combined geochronological, geochemical, and petrographic studies of these six particles. We hoped that additional analyses might pin down the age of the Crisium Basin; as it turned out, our results cast some doubt on the 3.84 Ga age for Crisium.

REGIONAL GEOLOGICAL SETTING

The Luna 20 spacecraft landed in the highlands near Apollonius Crater at about 3.5°N, 56.5°E, the easternmost sample return from the Moon. This region of the Moon consists of rugged terrae external to the rim of the Crisium Basin (Fig. 1), one of the most unusual and least understood multiring basins on the Moon (Wilhelms, 1987; Spudis et al., 1989). Although definitive surface textures are not apparent, the circum-Crisium highlands have been generally interpreted as representing deposits from the Crisium-forming impact. The highlands in this area consist of an irregular step-and-platform topography; interplatform areas appear to be filled with highland (high albedo) smooth plains (Spudis et al., 1989).

The Luna 20 site is on the inner, continuous deposits of the Crisium Basin (Fig. 2); its relation to the basin topographic rim is uncertain. Wilhelms (1987) interprets the Crisium Basin as being 1100 km in diameter; if this is correct, then the Luna 20 site is inside the basin and some quantity of basin impact-melt rock derived from the basin melt sheet should be present. Spudis et al. (1989) interpret the Crisium Basin as being only 740 km in diameter; if this is correct then the Luna 20 site lies entirely outside the basin rim and any impact-melt samples

¹Lunar and Planetary Laboratory, University of Arizona, Tucson, AZ 85721

²Branch of Astrogeology, U.S. Geological Survey, Flagstaff, AZ 86001

³Now at Lunar and Planetary Institute, Houston, TX 77058

⁴Planetary Geosciences Division, Department of Geology and Geophysics, School of Ocean and Earth Science and Technology, University of Hawaii, Honolulu, HI 96822

⁵McDonnell Center for Space Sciences, Washington University, St. Louis, MO 63130

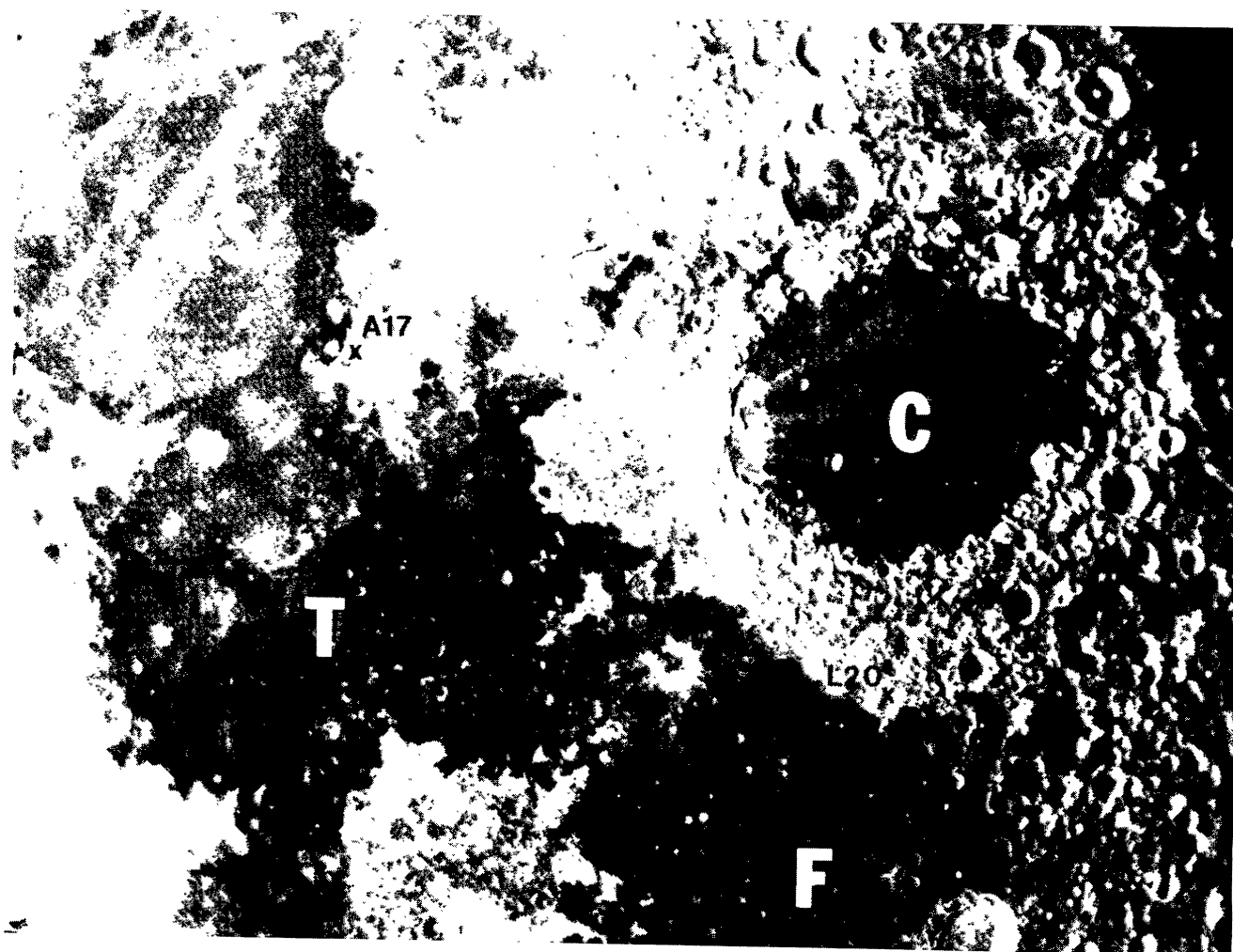


Fig. 1. Regional view, showing Mare Crisium (C), Mare Serenitatis (S), Mare Tranquillitatis (T), and Mare Fecunditatis (F). The locations of the Luna 20 (L20, southwest of Mare Crisium) and Apollo 17 (A17, east of Mare Serenitatis) landing sites are marked. Rectified, Earth-based photograph (Lunar and Planetary Lab., Univ. of Arizona, from Lick Observatory photograph).

from Crisium in the Luna 20 collection are derived from ejected melt deposits rather than the basin melt sheet. In general, the soil returned by the Luna 20 spacecraft is rock-poor, and impact melts are not common; this relation may indicate that the site is outside the basin rim and any Crisium Basin melt is present in minor quantities.

PROCEDURES

Six samples that appeared, on the basis of visual inspection, to be impact melts were selected for analysis. Thin sections were made of the two largest fragments, designated A and B. For the remaining samples, there was not enough material to both make thin sections and obtain chemical and chronological information, so no thin sections were made.

Broad-beam microprobe analyses were done on clasts A and B, with an ARL-EMX electron microprobe using crystal spectrometers. Ten 100- μm points were analyzed on each

fragment. Large mineral clasts were avoided, but not all clasts could be avoided on clast-rich sample 22023,3,B. Microprobe data were corrected by procedures described by *Bower et al.* (1977).

Clasts C through F and the remaining portions of clasts A and B were irradiated at the University of Missouri Research Reactor for 116 hours in May 1989, receiving a nominal fluence of 2×10^{19} neutrons/cm². Spatial variations in neutron fluence were monitored with Co-doped Al wires placed adjacent to each sample. Measured variations from the mean were less than 0.3% (comparable to the uncertainties in wire masses) and random, so all samples were assumed to have received the same fluence, with a $\pm 0.3\%$ uncertainty. The absolute fluence was calibrated with NBS flyash, CaF₂, and hornblende (hb3gr) monitors.

Radioassay and data reduction procedures for the instrumental neutron activation analysis (INAA) were similar to those described by *Korotev* (1991).

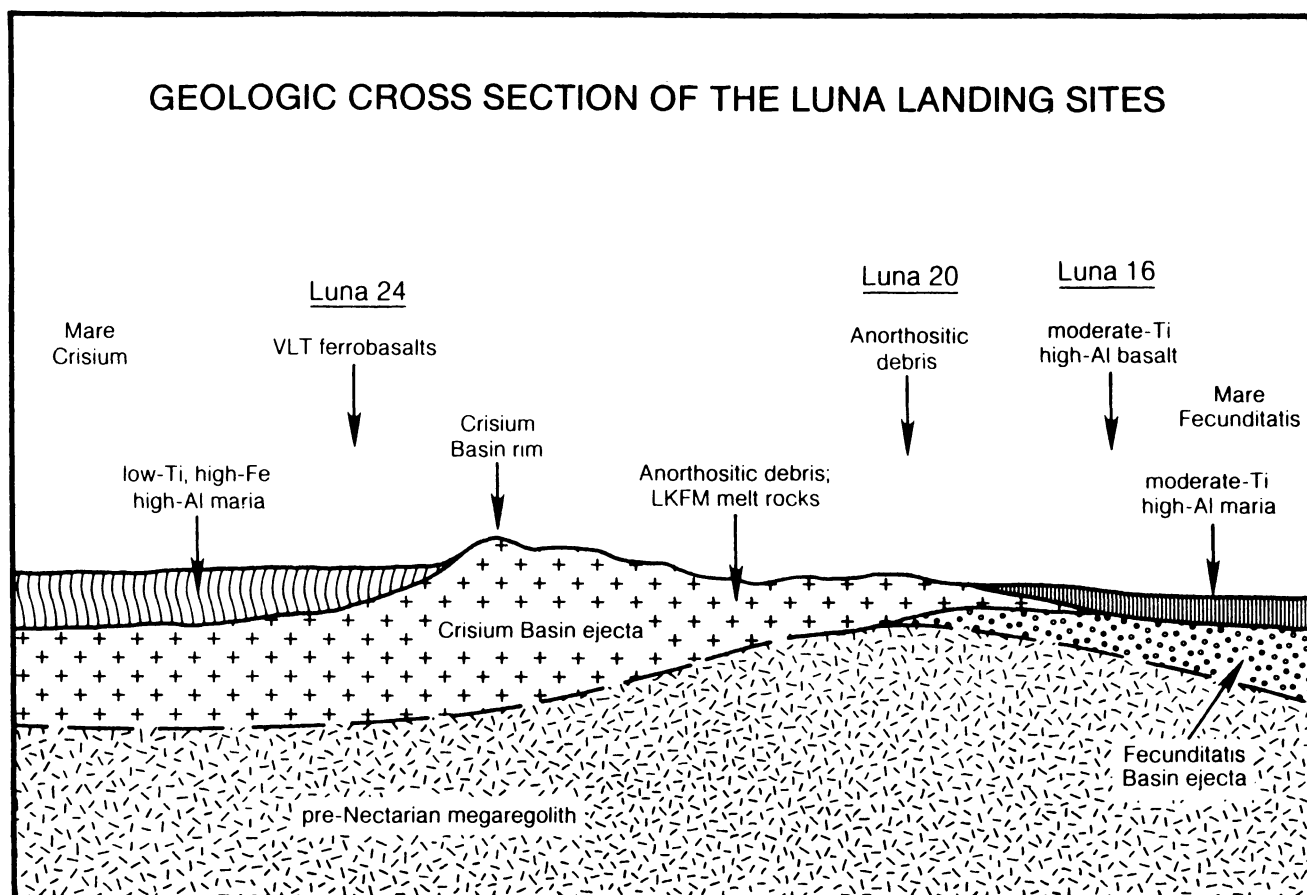


Fig. 2. Cross section showing the regional geologic relations in the vicinity of the Luna landing sites. The Luna 20 site is on continuous deposits associated with the Crisium Basin. From *Heiken and Vaniman* (1991).

Argon analyses were performed on a high-sensitivity static mass spectrometer (*Hobenberg*, 1980). Gas was extracted by stepwise heating using a resistance-heated tungsten coil. Coil temperatures during extraction are estimated to be 200°C to 300°C hotter than the samples themselves, due to imperfect thermal coupling. Noble gases were purified by sequential exposure to three freshly deposited Ti films. Because of concerns about the limited dynamic range of the mass spectrometer's ion-counting system, each gas sample was split into two unequal (4:1) portions, and each portion was analyzed. As it turned out, all gas samples were measurable, so the quoted results are based on the larger fraction in every case. However, the data for the smaller fractions were also analyzed, and no systematic differences were discovered.

Argon Data Reduction

Argon data were corrected for procedural and instrumental blanks, radioactive decay, reactor interferences, and spallation.

A series of blanks, at temperatures spanning the range of extraction temperatures, was run before the first sample, and then two blanks, one at 800°C and one at 1800°C, were run after each sample. We have found that our blanks can be

decomposed into three components: atmospheric, Cl- and HCl-derived, and a blank of unknown origin (perhaps $C_6H_6^{++}$) at mass 39. The atmospheric blank is constant with temperature for coil temperatures through 1600°C, then increases with temperature. For each sample, the last low-temperature blank run before it was used for corrections at $T \leq 1600^\circ C$, with a 20% uncertainty (comparable to the typical variations from day to day) assigned to the amount. Blanks ranged from about 5×10^{-11} to 1×10^{-10} cm³STP of ⁴⁰Ar. The average of the most recent 800°C and 1800°C blanks was used for the 1700°C blank, with a 50% uncertainty assigned. The Cl- and HCl-derived blanks varied by about 10% in amount, but were constant in composition at masses 35, 36, 37, and 38, so corrections were made by assuming that all the signal at mass 35 was from this component. The blank at mass 39 was 5×10^{-14} cm³STP, with a 30% uncertainty.

After correcting for blanks, ³⁷Ar amounts were corrected for radioactive decay, with all corrections made to the date of analysis of the calcium fluoride monitor. Argon-39 was not corrected for decay, because all samples were run within five days of the analysis of the hornblende monitor, so the error introduced is less than four parts in 10⁵. Table 1 contains the Ar data for each sample, corrected for blanks and decay.

TABLE 1. Argon data for Luna 20 impact melts.

Temp. °C	^{36}Ar 10^{-8} cm ³ STP/gm	Isotopic Ratios ($^{36}\text{Ar} = 100$)				"Corrected" [†]	
		^{37}Ar	^{38}Ar	^{39}Ar	^{40}Ar	^{39}Ar	^{40}Ar
<i>Luna 22023,3,A (1.551 mg)</i>							
800	18.0	0.42 ±0.10	20.98 ±0.11	0.381 ±0.013	387. ±6.	0.364 ±0.014	394. ±6.
900	94.1	0.407 ±0.024	20.20 ±0.09	0.1692 ±0.0032	357.0 ±1.6	0.1486 ±0.0035	361.0 ±1.6
1000	333.4	0.330 ±0.006	20.03 ±0.07	0.0999 ±0.0008	249.5 ±0.9	0.0826 ±0.0009	261.9 ±0.9
1100	727.8	0.218 ±0.003	19.97 ±0.07	0.0913 ±0.0005	173.7 ±0.6	0.0801 ±0.0005	175.3 ±0.6
1150	123.6	0.594 ±0.024	21.99 ±0.08	0.2747 ±0.0019	176.9 ±1.0	0.2483 ±0.0024	181.3 ±1.0
1220	63.5	0.684 ±0.036	22.58 ±0.09	0.4057 ±0.0048	188.6 ±1.8	0.379 ±0.005	194.3 ±1.8
1300	153.1	0.232 ±0.024	20.17 ±0.08	0.1346 ±0.0013	207.0 ±1.0	0.1232 ±0.0019	209.3 ±1.0
1400	381.8	0.054 ±0.007	19.34 ±0.07	0.0370 ±0.0004	212.7 ±0.7	0.0342 ±0.0006	213.6 ±0.8
1500	77.7	3.19 ±0.06	35.12 ±0.13	2.207 ±0.010	262.1 ±1.6	2.323 ±0.012	299.5 ±1.9
1600	1.4	14.6 ±1.4	86.3 ±0.6	3.59 ±0.12	607. ±73.	5.79 ±0.29	126. ±15.
1700	0.4	26. ±9.	141. ±6.	5.84 ±0.42	500. ±1500.	73. ±48.	900. ±2600.
Total	1974.8	0.388 ±0.009	20.77 ±0.05	0.2005 ±0.0048	211.8 ±1.0		
<i>Luna 22023,3,B (0.465 mg)</i>							
800	1.8	0.1 ±3.6	45.8 ±1.0	2.48 ±0.20	680. ±10.	3.12 ±0.36	8670. ±240.
950	6.2	3.6 ±1.0	50.78 ±0.49	2.15 ±0.10	2940. ±60.	2.58 ±0.15	3900. ±80.
1120	8.8	4.6 ±0.8	57.87 ±0.36	2.96 ±0.07	2649. ±39.	3.86 ±0.12	3780. ±60.
1250	2.5	10.1 ±2.7	113.0 ±1.7	8.17 ±0.34	6920. ±130.	27.2 ±1.9	24700. ±1300.
1400	3.1	5.5 ±2.1	78.7 ±0.6	5.34 ±0.17	6060. ±100.	9.30 ±0.39	11190. ±210.
1600	65.9	9.09 ±0.10	98.64 ±0.41	5.01 ±0.03	4568. ±17.	11.59 ±0.18	11730. ±170.
1700	2.4	8.8 ±3.4	106.4 ±2.6	4.69 ±0.23	3700. ±800.	12.7 ±1.1	11100. ±2400.
1800	1.1	12. ±6.	132.3 ±2.7	5.73 ±0.32	5210. ±490.	38. ±7.	39000. ±7000.
Total	91.8	8.04 ±0.22	90.80 ±0.47	4.67 ±0.03	4420. ±28.		
<i>Luna 22023,3,C (0.385 mg)</i>							
800	78.9	0.15 ±0.10	19.94 ±0.09	0.164 ±0.005	502.1 ±3.1	0.157 ±0.008	506.7 ±3.1
900	252.5	0.107 ±0.031	19.32 ±0.08	0.0962 ±0.0025	348.2 ±1.4	0.0907 ±0.0030	349.7 ±1.4
950	581.0	0.068 ±0.014	18.85 ±0.07	0.0537 ±0.0009	223.3 ±0.8	0.0500 ±0.0012	223.4 ±0.8
1000	550.0	0.063 ±0.014	19.19 ±0.07	0.0555 ±0.0010	150.8 ±0.6	0.0523 ±0.0013	151.3 ±0.6
1050	1439.5	0.067 ±0.005	19.65 ±0.07	0.0480 ±0.0005	102.3 ±0.4	0.0446 ±0.0006	102.99 ±0.37
1100	910.9	0.051 ±0.009	19.73 ±0.08	0.0385 ±0.0009	99.2 ±0.4	0.0360 ±0.0011	99.92 ±0.41
11150	291.8	0.102 ±0.031	20.56 ±0.09	0.0927 ±0.0024	165.4 ±0.9	0.0883 ±0.0030	167.7 ±0.9
1225	256.4	0.310 ±0.030	22.74 ±0.09	0.2108 ±0.0031	257.9 ±1.2	0.1999 ±0.0036	265.9 ±1.2

TABLE 1. (continued).

Temp. °C	^{36}Ar 10^{-8} cm ³ STP/gm	Isotopic Ratios ($^{36}\text{Ar} = 100$)					
		"Uncorrected"*				"Corrected"†	
		^{37}Ar	^{38}Ar	^{39}Ar	^{40}Ar	^{39}Ar	^{40}Ar
<i>Luna 22023,3,C (0.385 mg) continued</i>							
1400	921.1	0.058	19.75	0.0400	165.0	0.0371	166.2
		±0.009	±0.08	±0.0008	±0.6	±0.0009	±0.6
1450	270.4	0.062	19.88	0.0494	170.9	0.0464	172.4
		±0.028	±0.08	±0.0016	±1.0	±0.0022	±1.0
1525	155.6	1.09	32.54	0.598	589.2	0.602	658.3
		±0.05	±0.13	±0.008	±2.4	±0.009	±2.8
1600	4.0	5.9	73.1	2.23	1860.	3.26	3180.
		±2.0	±0.8	±0.10	±50.	±0.25	±100.
1700	1.9	8.	108.0	2.53	1300.	6.5	4100.
		±5.	±3.1	±0.25	±900.	±1.3	±2800.
Total	5713.9	0.112	20.16	0.0772	173.6		
		±0.005	±0.04	±0.0011	±1.4		
<i>Luna 22023,3,D (0.528 mg)</i>							
800	37.2	0.14	21.68	0.610	979.	0.616	1002.
		±0.17	±0.18	±0.014	±7.	±0.017	±7.
900	331.1	0.122	20.60	0.1588	572.9	0.1543	581.1
		±0.018	±0.08	±0.0025	±1.9	±0.0028	±2.0
950	342.6	0.085	20.12	0.0817	416.6	0.0778	420.9
		±0.018	±0.08	±0.0023	±1.5	±0.0025	±1.5
1000	927.1	0.080	20.31	0.0436	258.8	0.0397	261.9
		±0.006	±0.07	±0.0005	±0.8	±0.0007	±0.9
1050	1433.7	0.099	21.29	0.0355	148.3	0.0307	151.2
		±0.005	±0.08	±0.0003	±0.5	±0.0004	±0.5
1100	557.6	0.166	23.32	0.0554	144.2	0.0479	149.4
		±0.010	±0.09	±0.0009	±0.6	±0.0011	±0.6
1150	175.1	0.773	39.60	0.2145	233.8	0.205	277.7
		±0.035	±0.16	±0.0041	±1.3	±0.005	±1.6
1200	94.0	1.28	54.14	0.358	298.0	0.395	407.6
		±0.07	±0.23	±0.005	±2.0	±0.009	±3.2
1275	95.8	0.39	29.70	0.1253	185.7	0.113	202.5
		±0.06	±0.24	±0.0039	±2.1	±0.006	±2.3
1350	196.7	0.138	23.01	0.0499	184.4	0.0437	190.5
		±0.028	±0.09	±0.0018	±1.0	±0.0025	±1.1
1425	295.8	0.087	21.35	0.0259	188.4	0.0216	192.2
		±0.019	±0.09	±0.0013	±0.8	±0.0017	±0.8
1500	42.5	2.71	94.46	0.664	487.1	1.220	1150.
		±0.15	±0.44	±0.010	±4.2	±0.034	±18.
1600	6.5	4.1	137.4	1.29	932.	11.2	9800.
		±0.9	±1.1	±0.05	±25.	±1.5	±1100.
1700	1.9	2.6	145.1	1.11	200.	25.	6000.
		±3.4	±3.0	±0.13	±700.	±19.	±19000.
Total	4537.8	0.193	23.75	0.0804	244.1		
		±0.006	±0.09	±0.0011	±2.2		
<i>Luna 22023,3,E (0.254 mg)</i>							
900	19.1	0.5	18.78	0.029	952.	0.001	952.
		±0.6	±0.09	±0.028	±25.	±0.043	±25.
1000	105.9	0.14	18.48	0.033	251.	0.025	251.4
		±0.12	±0.14	±0.005	±5.	±0.008	±4.6
1100	180.8	0.00	19.32	0.022	114.	0.0229	114.0
		±0.07	±0.07	±0.004	±3.	±0.0036	±2.7
1200	48.0	0.00	20.06	0.056	106.	0.056	107.
		±0.25	±0.12	±0.011	±10.	±0.011	±10.
1300	6.7	0.0	21.0	0.17	170.	0.18	180.
		±1.7	±0.6	±0.08	±70.	±0.08	±70.
1400	10.9	0.9	21.04	0.31	148.	0.27	151.
		±1.2	±0.14	±0.05	±44.	±0.09	±44.
1500	16.5	2.3	26.26	1.13	157.	1.07	166.
		±0.9	±0.38	±0.06	±29.	±0.08	±31.
1600	6.5	23.4	80.4	7.84	240.	12.5	450.
		±2.8	±1.5	±0.22	±70.	±0.6	±140.
1700	11.9	42.0	136.2	15.72	300.	139.	3100.
		±2.3	±1.8	±0.28	±200.	±23.	±2100.

TABLE 1. (continued).

Temp. °C	^{36}Ar 10^{-8} cm ³ STP/gm	Isotopic Ratios ($^{36}\text{Ar} = 100$)				"Corrected" [†]	
		^{37}Ar	^{38}Ar	^{39}Ar	^{40}Ar	^{39}Ar	^{40}Ar
<i>Luna 22023,3,E (0.254 mg) continued</i>							
1800	1.6	47.93 10.44	151.43 ±5.28	16.979 ±0.804	365. ±877.	‡	‡
Total	407.9	1.95 ±0.15	24.42 ±0.24	0.734 ±0.031	200. ±8.		
<i>Luna 22023,3,F (0.524 mg)</i>							
800	1.4	-2.5 ±3.8	25.3 ±0.6	1.29 ±0.24	2790. ±100.	1.36 ±0.25	2930. ±100.
900	5.9	1.0 ±0.9	26.83 ±0.24	1.33 ±0.06	1381. ±26.	1.36 ±0.08	1472. ±27.
1000	33.8	0.30 ±0.16	22.25 ±0.12	0.619 ±0.015	682. ±5.	0.619 ±0.018	701. ±5.
1100	114.2	0.209 ±0.047	21.06 ±0.10	0.324 ±0.008	366.6 ±1.9	0.319 ±0.009	373.1 ±2.0
1200	100.9	0.29 ±0.05	23.04 ±0.10	0.507 ±0.009	608.4 ±2.5	0.507 ±0.010	628.8 ±2.6
1300	130.4	0.187 ±0.043	21.34 ±0.10	0.320 ±0.007	635.7 ±3.0	0.316 ±0.008	648.5 ±3.1
1400	451.0	0.070 ±0.012	20.00 ±0.08	0.1325 ±0.0021	467.3 ±1.5	0.1298 ±0.0022	471.7 ±1.6
1450	89.8	0.13 ±0.06	20.94 ±0.10	0.202 ±0.005	503.2 ±2.6	0.198 ±0.006	511.7 ±2.7
1500	22.6	3.19 ±0.26	63.92 ±0.30	6.27 ±0.06	5558. ±20.	9.31 ±0.10	8480. ±50.
1550	53.8	7.64 ±0.23	123.7 ±0.5	15.03 ±0.07	12988. ±50.	73.5 [§] ±2.7	65300. [§] ±2400.
1600	0.7	1. ±9.	144.9 ±2.2	11.8 ±0.6	10400. ±190.	§	§
1700	2.8	8.6 ±2.1	149.7 ±1.8	9.24 ±0.22	7470. ±260.	§	§
1800	0.9	6.9 ±7.3	144.9 ±3.4	3.92 ±0.31	2900. ±600.	94. [§] ±68.	78000. [§] ±58000.
Total	1008.5	0.642 ±0.033	27.89 ±0.33	1.217 ±0.046	1322. ±38.		

* Isotopic composition of Ar contained in the samples after irradiation. Data in these columns have been corrected for instrumental mass discrimination, memory/pumpout, and blanks, and ^{37}Ar and ^{39}Ar have been corrected for decay that occurred between the time the CaF_2 monitor was analyzed and the time of sample analysis.

† Isotopic composition of trapped and K-derived Ar, derived from previous columns by correcting for reactor interferences and spallation-produced Ar.

‡ After spallation correction, ^{36}Ar , like ^{40}Ar , is blank level.

§ >75% of the ^{36}Ar in the 1550°C extraction, and >95% in the 1600°-1800°C extractions, attributable to spallation. Spallation-corrected $^{36}\text{Ar}/^{40}\text{Ar}$ and $^{39}\text{Ar}/^{40}\text{Ar}$ ratios are: 1550: 0.00153(6), 0.001125(3); 1600: 0.00037(18), 0.00113(7); 1700: 0.00000(21), 0.001175(43); 1800: 0.0013(10), and 0.00120(35).

All uncertainties are 1σ .

Neutron-induced interferences from Cl, Ca, and K are potentially present, but we corrected only for Ca. All the ^{37}Ar remaining after the blank correction is assumed to be Ca-derived. Corrections for Ca-derived Ar were based on the $^{36}\text{Ar}/^{37}\text{Ar}$ and $^{39}\text{Ar}/^{37}\text{Ar}$ ratios (0.0253 ± 0.0001 and 0.0548 ± 0.0001) of the calcium fluorite monitor and the $^{38}\text{Ar}/^{37}\text{Ar}$ ratio (0.0094 ± 0.0047) given by *Turner et al.* (1978). We did not apply any corrections for Cl, which can produce ^{38}Ar , since plots of $^{38}\text{Ar}/^{36}\text{Ar}$ vs. $^{37}\text{Ar}/^{36}\text{Ar}$ contained no evidence for anything more than a two-component mixture of trapped and Ca-derived (spallation + reactor products) Ar. We did not correct for K interferences, either, since the corrections based on the $^{38}\text{Ar}/^{39}\text{Ar}$ and $^{40}\text{Ar}/^{39}\text{Ar}$ ratios given by *Kennedy* (1981) would always be less than 20% of the 1σ uncertainty.

Finally, spallogenic Ar was removed by assuming that the $^{38}\text{Ar}/^{36}\text{Ar}$ ratio represents a two-component mixture of trapped (0.188) and spallogenic (1.5) Ar. Cosmic-ray exposure ages (Table 2) were computed based on the $^{38}\text{Ar}/^{37}\text{Ar}$ ratio determined from plots of $^{38}\text{Ar}/^{36}\text{Ar}$ vs. $^{37}\text{Ar}/^{36}\text{Ar}$. The $^{38}\text{Ar}/^{37}\text{Ar}$ ratio derived by component decomposition is identical, within 1σ . We used a production rate of 1.0×10^{-8} cm³STP $^{38}\text{Ar}/\text{gCa}/\text{Ma}$, obtained by averaging the production rate for the top 200 g/cm² of shielding (*Hohenberg et al.*, 1978). Our production rate is within 25% of the rate for any shielding between about 4 and 200 g/cm². Note that *Podosek et al.* (1973) used a production rate 40% higher, hence the values in Table 2 for their samples are 40% higher than the values they quoted.

TABLE 2. Argon results—summary.

Sample	Texp (Ma)	⁴⁰ Ar- ³⁹ Ar systematics				CaO (wt%)	K ₂ O (wt%)
		Temp.* (#)	% of ³⁹ Ar'	⁴⁰ Ar/ ³⁶ Ar	Age† (Ga)		
22023,3 (this study)							
A	340 ±90	1300-	52	2.10	0.519	15.4	0.09
		1500 (3) 1600 (model)	1	±0.01 ≡2 ±1	±0.011 1.72 ±0.19	±1.5	±0.01
B	680 ±270	1600 (model)	81	≡2	4.087	14.3	0.09
C	1010 ±250	1400-	35	1.34	3.879	13.5	0.11
		1700 (5)		±0.01	±0.031	±1.4	±0.01
D	2080 ±520	1100-	31	1.13	3.687	17.6	0.08
		1275		±0.01	±0.037	±1.8	±0.01
		1425-	12	1.75	3.751		
		1600 (3) 1500-	10	±0.02	±0.041		
E	180 ±50	1600 (2) 1100-	90	1.0	3.86	16.0	0.06
		1700 (7)		±0.03	±0.11	±1.6	±0.01
F	1010 ±250	1300-	90	3.55	3.895	13.0	0.30
		1800 (8)		±0.02	±0.017	±1.3	±0.03
<i>Podosek et al. (1973)</i>							
22006	640 ±160	770-	90	≡2.15	3.847		
		1590 (7)		±0.22	±0.023		
22007	930 ±230	885-	83	2.15	3.853		
		1460 (4)		±0.22	±0.024		

* Extraction temperatures of data points included in isochron in °C (number of temperature steps in parentheses). Note that for this study, the temperature of the heating coil (which is listed) is typically 200°–300°C hotter than the sample itself.

† Uncertainty includes 1% uncertainty in calibration of hb3gr monitor for this study, 1.5% uncertainty for *Podosek et al. (1973)*, 0.3% uncertainty in neutron fluence relative to monitor.

PETROGRAPHY

22023,3,A

This fragment (Fig. 3a) is a clast-poor impact-melt rock. It has elongated plagioclase laths up to 200 μm long and 10 μm wide. Matrix between the laths consists of glass and a quench-textured chain-like mafic mineral, probably pyroxene. A small amount (<1%) of euhedral Mg,Al spinel is also present. Numerous small (1–5 μm) metallic grains are present throughout the fragment; there is also one oval metal grain 90 μm along the longest axis. Clasts make up only about 5% of the breccia and are all equant plagioclase, averaging about 100 μm across.

22023,3,B

This is a fine-grained, clast-rich impact-melt breccia (Fig. 3b). The matrix consists of small (20–50 μm) pyroxene grains that enclose plagioclase grains, a small percentage of which are lath shaped. Clasts make up 25% of the fragment and range in size from 10 to 200 μm. Most are plagioclase, but olivine and pyroxene are also present. One polymineralic clast is present. It is only 60 μm across and consists of olivine, plagioclase, and ilmenite in a fine-grained intergrowth surrounding one relatively large (30 μm across) olivine grain.

Other Particles

Because of the limited amount of sample, no thin sections were made. Nevertheless, the fragments appeared macroscopically to be fine-grained, crystalline rocks, probably impact melts. All contained clasts, and could be distinguished easily from regolith breccias.

Bulk Compositions (A and B)

Broad-beam analyses of matrix portions of both fragments are given in Table 3. This gives major elements not analyzed by the INAA procedure. Agreement with both the INAA and the Ar-derived elemental abundances is generally good. Both fragments are more aluminous than low-K Fra Mauro (LKFM) basalt, a common highlands rock type usually associated with basin ejecta elsewhere on the Moon (e.g., *Spudis, 1984*).

ARGON CHRONOLOGICAL RESULTS

The K-Ar systematics of the six samples have certain things in common. Four of the six (A, C, D, and E) have bulk ⁴⁰Ar/³⁶Ar ratios of less than 3, even after correction for spallation. The ⁴⁰Ar/³⁶Ar ratio of the trapped component [presumably a mixture of solar wind, “orphan” ⁴⁰Ar (*Yaniv and Heymann, 1972*), and perhaps some radiogenic ⁴⁰Ar that was mobilized

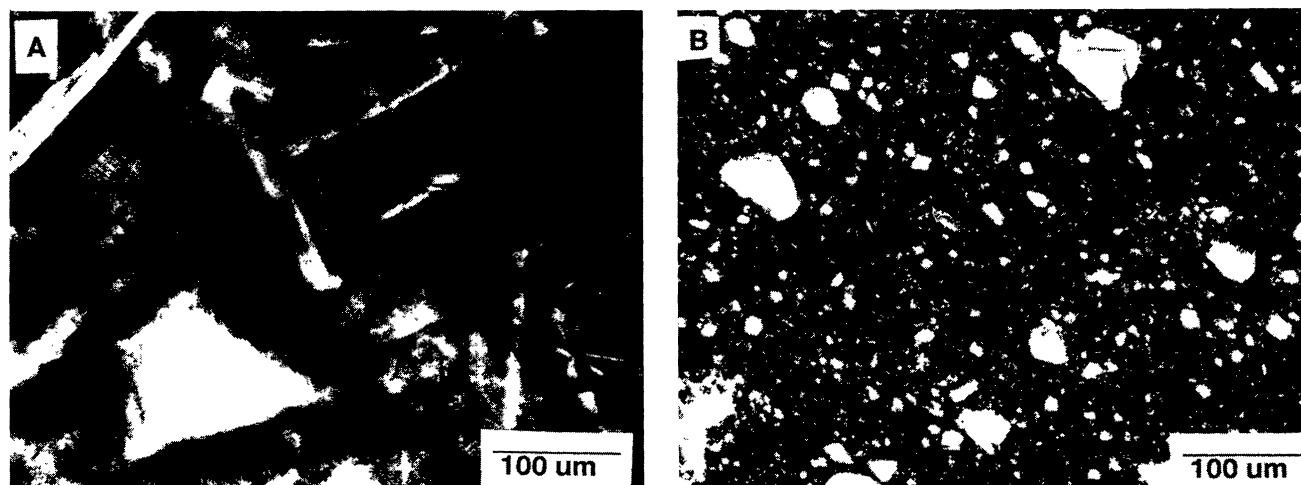


Fig. 3. Photomicrographs of Luna 20 impact-melt rocks 22023,3 A and B. (a) Fragment A, a clast-poor impact-melt rock. Elongate plagioclase phenocrysts occur throughout the sample. Clasts, such as the plagioclase grain shown in the lower left, constitute only 5% of the rock. The mesostasis between the plagioclase laths consists of glass and chain-like pyroxene. (b) Fragment B, a fine-grained, clast-rich impact-melt breccia. Clasts (essentially all the visible crystals in this photograph) make up at least 25% of the fragment; most are plagioclase. The matrix consists of small pyroxene grains that enclose smaller plagioclase.

TABLE 3. Broad-beam microprobe analyses of Luna 20 fragments.

	22023,3,A		22023,3,B	
	Microprobe	Other*	Microprobe	Other*
SiO ₂	44.2		44.5	
TiO ₂	0.18		0.36	
Al ₂ O ₃	27.4		25.7	
Cr ₂ O ₃	0.11	0.10	0.13	0.15
FeO	3.4	3.7	5.2	6.2
MnO	0.05		0.10	
MgO	6.6		5.7	
CaO	15.4	15.5,15.4	15.6	14.6,14.3
Na ₂ O	0.43	0.46	0.35	0.39
K ₂ O	0.06	0.09	0.07	0.09
Total	97.83		97.71	
Mg [#]	78		66	

* INAA data (Table 4), except for K₂O and second CaO number, which are from Ar (Table 2).

but not lost during formation of the rock] is thus crucial to the interpretation, so we have used three-isotope plots (Fig. 4) rather than the more traditional plateau plots. On the three-isotope plots, there always appears to be excess ⁴⁰Ar in the low-temperature steps (also observed by *Podosek et al.*, 1973, and *Cadogan and Turner*, 1977). This could be the result of incorporation of terrestrial contamination, dominated by ⁴⁰Ar, or it could be the result of incorporation of an Ar component that was not available when the higher-temperature sites underwent isotopic closure [e.g., a component that was implanted after solidification (*Podosek et al.*, 1973) or one that evolved during the later stages of melt cooling (*Bottomley et al.*, 1990)]. Another, less likely, possibility is recoil of ³⁹Ar from fine-grained, low-temperature sites (in several cases, more than 90% of the ³⁹Ar would have to be lost to reconcile a low-temperature point with the apparent isochron).

Despite these potential complications, in most cases the high-temperature extractions are consistent with a single isochron representing most of the ³⁹Ar (and, by inference, the K). The presence of an isochron suggests that the K-Ar system (for those extractions that plot on the isochron) can be described by a single age and a single trapped ⁴⁰Ar/³⁶Ar ratio. The results of these isochrons are summarized in Table 2. The ages differ from those reported in a preliminary abstract (*Swindle et al.*, 1990) as a result of an incorrect constant used in the preliminary calculations.

The isochrons for E and F are the best-defined, involving several points representing >90% of the ³⁹Ar. Each isochron appears to be dominated by a single point (1600°C for E and 1550°C for F), but in each case, fitting a line to the data without the "dominant" point gives a result that differs by less than the uncertainty quoted in Table 2. Since the age of F is crucial to our interpretations, we have included a conventional plateau plot, after subtracting a trapped ⁴⁰Ar/³⁶Ar determined by the isochron intercept (Fig. 5). Incidentally, even though the trapped ⁴⁰Ar/³⁶Ar ratio in F is the highest observed, the four highest-temperature extractions are sufficiently radiogenic that the trapped component is insignificant (a trapped ratio of 0 would raise the apparent ages of the 1550°-1800°C points by less than 0.5σ). The isochron for C is reasonably well defined, but it contains only 35% of the ³⁹Ar.

For A and B, there are no multiextraction isochrons, but there is a significant amount of information available. For A, the ⁴⁰Ar/³⁶Ar ratio is virtually independent of the ³⁹Ar/³⁶Ar ratio, indicating a young age (about 0.5 Ga) with a trapped ⁴⁰Ar/³⁶Ar ratio of about 2. The 1600°C extraction gives a model age of about 1.7 Ga, suggesting incomplete outgassing at the time of formation. For B, 80% of the ³⁹Ar came off in a single step (1600°C) with a high enough ³⁹Ar/³⁶Ar ratio that the ⁴⁰Ar/³⁶Ar ratio of the trapped component is insignificant

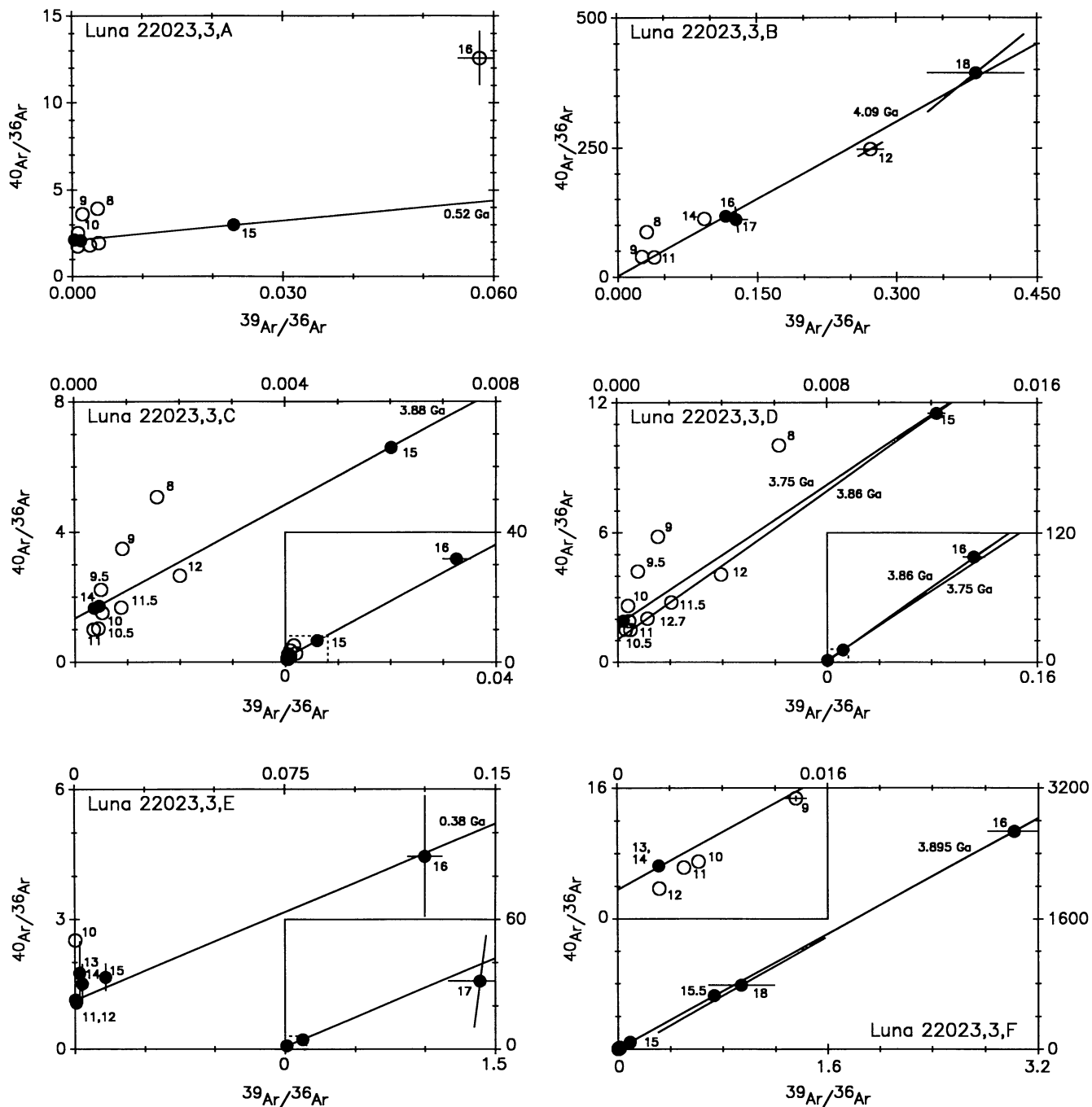


Fig. 4. Three-isotope plots for irradiated Luna 20 impact melts. In these plots, the trapped $^{40}\text{Ar}/^{36}\text{Ar}$ ratio is given by the ordinate-intercept, while the age is proportional to the slope. Solid lines denote the isochrons listed in Table 2, and are fit to the solid symbols. Numbers next to points denote extraction temperatures in hundreds of degrees C. Except where plotted, 1σ error bars are smaller than the symbols. In some cases where the uncertainty in the amount of ^{36}Ar is the dominant uncertainty, the error bars are not parallel to the axes. In two plots (C and F), highly radiogenic 1700°C extractions, which would fall far off-scale to the upper right, are not plotted. In each case, the extraction is consistent with the fit line, within 1σ [model ages are $3.3 (+0.8, -1.5)$ Ga for C, 3.84 ± 0.06 Ga for F].

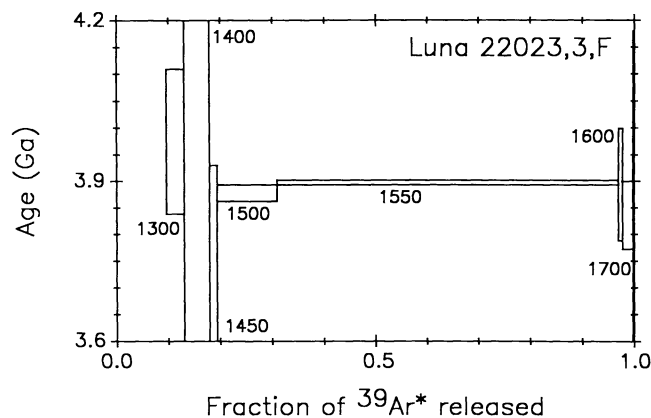


Fig. 5. $^{40}\text{Ar}/^{39}\text{Ar}$ plateau plot of apparent age for 22023,3,F. Horizontal line is at 3.895 Ga.

if it is in the range observed for the other samples. However, the dominance of a single step makes it impossible to detect subtleties like the incomplete outgassing apparently observed in A.

The case where the interpretation is most ambiguous is that of D (Fig. 4; Table 2). Fits to the 1100° - 1275°C extractions (four points, 3.69 Ga, line not plotted) and the 1425° - 1600°C extractions (three points, 3.75 Ga) give distinct lines—neither line passes within 1σ of a point falling on the other line, and neither contains more than 31% of the $^{39}\text{Ar}'$ released. Meanwhile, a line passing through two of the three points involved in the latter fit (1500° and 1600°C , 3.86 Ga) is more consistent with the 1100° - 1275°C extractions than with the 1425°C extraction. Rather than make a case for any of these being the best isochron, we conclude only that the age is 3.75 ± 0.11 Ga, an uncertainty large enough to encompass any of them.

We have also recalculated the ^{40}Ar - ^{39}Ar and cosmic-ray exposure ages of 22006 and 22007 reported by Podosek *et al.* (1973), using the currently recommended K-decay parameters (Steiger and Jäger, 1977) and our preferred spallogenic Ar production rates (see above). We have recomputed the ^{40}Ar - ^{39}Ar ages by averaging the ages for the indicated steps, weighting by amount of ^{40}Ar . This gives ages a few Ma older than those obtained by converting the rounded-off age (3.90 Ga) reported by Podosek *et al.* (1973).

In trying to discern time differences of less than 10^8 years, an understanding of the uncertainties in ages is imperative. Statistical uncertainties in the measurements of samples or monitors by either us or Podosek *et al.* (1973) are $<0.5\%$. Neutron-flux variations, which were monitored in both cases, are unlikely to cause an uncertainty larger than about 0.3%. Most of the uncertainty in each case comes from uncertainty in the $^{39}\text{Ar}/\text{K}$ production ratio, probably reflecting minor impurities in the hb3gr monitors (Turner *et al.*, 1971; Roddick, 1983). Podosek *et al.* (1973) assumed a $\pm 2\%$ uncertainty for the $^{39}\text{Ar}/\text{K}$ production ratio, based on the 2.4% variation they observed between two samples of the hb3gr monitor included in their irradiation. We believe such a large uncertainty is

probably too conservative. In nine other irradiations in which multiple samples of hb3gr were analyzed (Turner *et al.*, 1971, 1972, 1978; Alexander and Davis, 1974; Cadogan and Turner, 1977; Kennedy, 1981), the largest variation seen was 1.6%, and the typical variation was less than 1%. We did not analyze aliquots, but we did perform a stepwise analysis on our sample of hb3gr, and while we saw evidence for a lower $^{40}\text{Ar}/^{39}\text{Ar}$ ratio at the lowest extraction temperature, 96% of the ^{39}Ar was consistent with a single $^{40}\text{Ar}/^{39}\text{Ar}$ ratio (cf. Turner *et al.*, 1971). Although at least one of the hb3gr samples analyzed by Podosek *et al.* (1973) was clearly anomalous, we find it unlikely that their weighted mean would differ from the mean for hb3gr by more than 1.5%. Therefore, in Table 2, we have assigned a 1.5% uncertainty to the $^{39}\text{Ar}/\text{K}$ ratio for 22007 and 22006, and a 1% uncertainty for the samples we analyzed. The calculated $^{40}\text{Ar}/\text{K}$ ratio of F is 2.7% larger than that of 22007. Contemporaneous ages cannot be ruled out, but variations in the $^{40}\text{Ar}/\text{K}$ of hb3gr would have to be at the level of 2σ , or variations in any other parameter would have to be at a level of at least 5σ . For the two other samples in this study with comparable ages, that of C is indistinguishable from either 22007 or F, while D could be consistent with either or neither.

CHEMISTRY—COMPOSITIONAL CLUSTERS OF LUNA 20 IMPACT MELT

While impact melts show great textural diversity, they tend to be very homogeneous chemically; this relation has been used as a tool to relate impact melts in the lunar samples to specific impact events by recognizing compositional clusters and attempting to assign them to impact events known to be important in the geologic evolution of a given site (e.g., Ryder and Spudis, 1987). Because geologic control of lunar samples is very poor, we can never be sure that the event with which we associate a given melt rock is the correct one. Usually, an abundance of data on many samples in association with a relatively clear geologic context is required to give us some reasonable degree of confidence in such an interpretation (e.g., the Serenitatis Basin "melt sheet" at Apollo 17; see Wolfe *et al.*, 1981). In the absence of this, our interpretations of sample context and their relation to major lunar events become more conjectural. Furthermore, in dealing with submilligram samples, there is a real problem with sample homogeneity: A single clast can alter the bulk chemical composition significantly. However, the questions addressed are of such importance that we must at least attempt to understand them. In this spirit, we shall try to understand the Luna 20 impact melts in terms of their relation to major, regional events in this part of the Moon.

The results of INAA of our six Luna 20 impact melt fragments, in addition to published analyses of other Luna 20 melts, are shown for the petrologically significant elements Sc and Sm in Fig. 6 (INAA results for a suite of 26 elements in our samples are given in Table 4). For comparison, we include the observed fields of the two well-characterized groups of Apollo 17 impact melts, the poikilitic melts and the aphanites. Many authors consider the poikilitic melts to represent the Serenitatis Basin melt sheet (Dymek *et al.*, 1976; Warner *et al.*, 1976; Winzer *et al.*, 1977; Spudis and Ryder, 1981). The

aphanites at Apollo 17 are of less certain provenance, but considered by many (Wood, 1975; Dence et al., 1976; James et al., 1978; Wolfe et al., 1981) to also be related to the Serenitatis Basin. We also include the Apollo 16 VHA basalts, interpreted as the Nectaris melt sheet (Spudis, 1984). The composition of Luna 20 impact melts varies widely and compositional clustering is less apparent at this site than at the Apollo 15 site (Ryder and Spudis, 1987). However, at least two major clusters can be recognized; one includes samples C, D, and E (Fig. 6, "group 1") and the other significantly overlaps with both Apollo 17 poikilitic and aphanitic fields—this "cluster" includes the previously dated fragment 22007,1 (Podosek et al., 1973). Our own sample "F" may be included within this latter cluster, although it largely appears to be associated with some other, apparently nonmelt Luna 20 samples (Fig. 6).

Other impact melts appear to be more dispersed. The high Sc cluster at ~ 4 ppm Sm includes two melts analyzed by Smith et al. (1983) and the Luna 20 soil composition; these melts could represent local impacts into the soil. The two impact melts "A" and "B" are relatively isolated and each has a unique age (see Discussion); they probably represent distinct impacts near the site, widely separated in time.

In short, no clear, unambiguous pattern, in the manner of the Apollo 17 impact melts, emerges from these data. We tentatively identify a loose cluster (Group 1, Fig. 6) associated with three of our samples; this "group" may in fact represent several impacts as they do not form a very tight cluster based on the analysis of other elements. The small "group 2" falls within the Apollo 17 field and appears to possess good compositional coherence; unfortunately, these samples may not be related to the Crisium Basin, but rather to Serenitatis, as

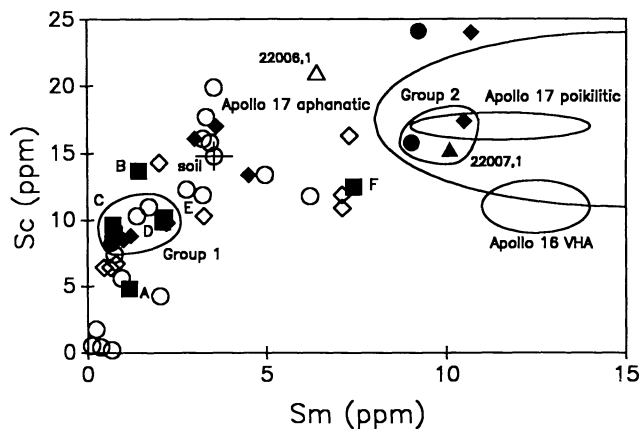


Fig. 6. Sc-Sm relations for a variety of Luna 20 rock fragments. Fields for the Apollo 17 poikilitic melt sheet, Apollo 17 aphanites, and Apollo 16 VHA basalts are shown for comparison. Samples known to be impact melts are plotted as solid symbols; some of the other samples may also be impact melts. Data are from this study (squares); Korotev and Haskin, 1988 (circles); Smith et al., 1983 (diamonds); and Laul and Schmütt, 1973 (triangles).

that basin is less than a basin diameter (750 km) from the Luna 20 site and some quantity of material from that impact might be expected.

Among our impact melts, sample "F" appears most likely to represent a significant event. It is clearly compositionally distinct from all other Luna 20 samples known to be impact melts (Fig. 6), with elevated rare-earth-element concentrations, yet it is also distinct from the nebulous "group 2" of Luna 20, which may be associated with the Serenitatis Basin. It is somewhat similar to Apollo 16 "VHA basalt" (Fig. 6), but overall is lower in rare earths. At least three additional particles (22007,5a, 22011,1b, and 22023,7M) are compositionally similar to impact melt "F" on this plot, although none of the three is an impact melt. In short, particle "F" is our current leading candidate for representing a major event, possibly the Crisium Basin. We discuss this possibility more fully below.

DISCUSSION

Our primary purpose in this study was to try to better define the age of the Crisium Basin impact. This means we must try to understand the age and provenance of each of the chemical groups observed, to try to identify the Crisium melt sheet. Figure 7 summarizes the ages that have been obtained for Luna 20 samples potentially related to impacts. We will discuss our ages in the framework of the basin chronology proposed by Wilhelms (1987), which is also shown in Fig. 7.

Impact Melt "Groups" at Luna 20

The indistinct "group 1" composition is not as homogeneous as the Apollo 17 poikilitic melts (Simonds, 1975; Winzer et al., 1977; Spudis and Ryder, 1981), but shows variation comparable to the aphanites from that site (Fig. 7). Three of our dated samples come from this melt group; C and D could be contemporaneous at 3.85 to 3.9 Ga, while particle E is a young sample (0.38 Ga; see below). This composition appears to be quite abundant at the Luna 20 site, as evidenced by the numerous other melts of this composition found in the samples by other workers (Fig. 6). Moreover, this "cluster" appears to form a continuum with more aluminous samples just below the field of group 1 (Fig. 6), a field that includes our sample A. They all appear to represent relatively common, upper crustal compositions in the region. We interpret this melt group as representing a variety of impacts, occurring at a variety of times throughout the history of the site. An alternative interpretation is that this group represents the Crisium Basin melt sheet, with E's age reset by a more recent cratering event. The ages of C and D are certainly compatible with the Crisium Basin in the chronology of Wilhelms (1987). However, the samples interpreted as the melt sheets of Nectaris, Serenitatis, and Imbrium do not have compositions that correspond with that of the local highlands crust in the vicinity of the Apollo sites (Spudis, 1984).

The Crisium Basin predates the Imbrium Basin (3.85 Ga) and possibly the Serenitatis (3.87 Ga) Basin (Wilhelms, 1987); the age of the "group 2" melts (3.85 ± 0.02 Ga) is thus only marginally consistent with a Crisium Basin origin. Wilhelms (1987) tentatively interpreted sample 22007,1 (a member of

TABLE 4. INAA results for particles from 22023,18.

	Mass mg	Na ₂ O %	CaO %	Sc μg/g	Cr μg/g	FeO %	Co μg/g	Ni μg/g	Sr μg/g	Zr μg/g	Cs μg/g	Ba μg/g	La μg/g	Ce μg/g	Nd μg/g	Sm μg/g	Eu μg/g	Tb μg/g	Yb μg/g	Lu μg/g	Hf μg/g	Ta μg/g	W μg/g	Ir ng/g	Au ng/g	Th μg/g	U μg/g
22023,18 A	1.544	0.457	15.5	4.81	698	3.73	19.6	226	170	31	0.06	37	2.55	6.4	4.	1.17	0.95	0.24	0.97	0.136	0.90	0.123	<2.	88	2.4	0.54	0.14
22023,18 B	0.461	0.389	14.6	13.7	1000	6.21	17.6	130	127	<80	0.11	38	2.97	7.8	—	1.43	0.81	0.34	1.39	0.193	0.94	0.10	<4.	3.5	3.5	0.48	0.22
22023,18 C	0.373	0.441	12.9	9.66	1360	6.91	26.4	245	139	<100	<0.15	21	1.44	3.9	—	0.71	0.67	0.16	0.65	0.094	0.53	0.07	<5.	9.4	4.8	0.17	<0.15
22023,18 D	0.521	0.315	16.7	9.87	733	4.62	10.7	99	152	87	0.06	55	4.47	11.5	6.	2.10	0.90	0.44	1.66	0.234	1.71	0.21	2.	5.3	<10.	0.77	0.20
22023,18 E	0.272	0.183	15.3	10.2	962	6.28	29.2	350	153	80	<0.15	64	4.53	11.8	8.	2.15	0.81	0.44	1.73	0.246	1.62	0.22	<2	21.	4.8	0.81	0.29
22023,18 F	0.523	0.459	13.3	12.5	1110	6.85	26.4	255	149	255	0.10	198	16.9	43.2	25	7.42	1.29	1.51	5.45	0.776	5.88	0.67	3.	6.2	4.2	2.70	0.77
Uncertainty (%)	1-2	1-2	1-2	1-2	1-2	1-2	1-2	10	12	15	30	12	1-2	2-5	20	1-2	2-4	3-5	2-4	2-4	2-5	5-10	40	30	30	3-6	20

Uncertainties are 1σ estimates of analytical precision.

— = no value reported.

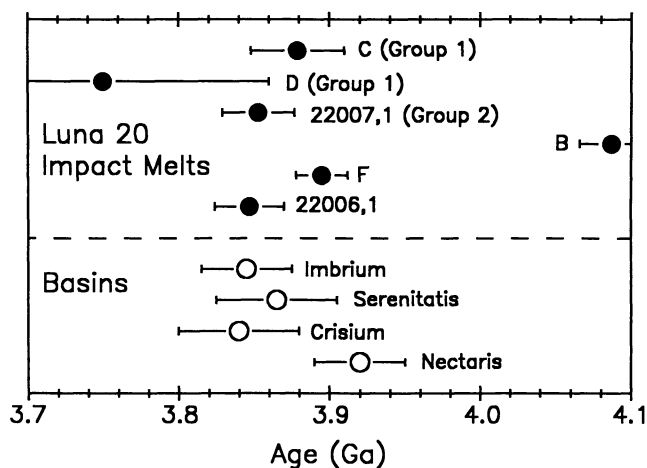


Fig. 7. Ages of Luna 20 impact melts (from Table 2; D is plotted as 3.75 ± 0.11 Ga, as discussed in text). Members of chemical groups identified in Fig. 6 are identified. At bottom of figure, the basin chronology of *Wilhelms* (1987) is plotted. Uncertainties quoted by *Wilhelms* are included, but note that relative ages are in the order Nectaris > Crisium > Serenitatis > Imbrium.

group 2) as Crisium Basin impact melt. Group 2 is LKFM in composition, and elsewhere on the Moon LKFM is associated with basin ejecta (e.g., *Spudis*, 1984). However, there are no regional exposures of LKFM in the vicinity of the Luna 20 site (*Davis and Spudis*, 1987) and a large, local crater origin for this sample is unlikely. Since the age and chemical composition of 22007,1 are so similar to those of Serenitatis, the group 2 melts could be fragments of that melt sheet.

Individual Impact Melts and Their Origins

Impact melt B, which is similar in composition to another Luna 20 sample (22008,2a of *Smith et al.*, 1983), gives a precise age (4.08 Ga) that is definitely older than the Imbrium, Serenitatis, and Nectaris impacts. It is distinctive chemically in that with a relatively low Mg' (66) and low concentrations of incompatible trace elements its composition does not resemble either the LKFM composition associated with the Imbrium and Serenitatis Basins (*Ryder and Spudis*, 1987) or the VHA basalt composition associated with the Nectaris Basin (*Spudis*, 1984). However, its composition is similar to those of some melt-rock clasts in feldspathic fragmental breccias from North Ray Crater at Apollo 16 (e.g., 67015,265 of *Marvin and Lindstrom*, 1983, and 67016,K of *Lindstrom and Salpas*, 1983). Also, it falls within the range of compositions obtained for bulk samples of meteorite Y-791197, a regolith breccia from an unknown lunar location (*Fukuoka et al.*, 1986; *Lindstrom et al.*, 1986; *Ostertag et al.*, 1986; *Warren and Kallemeyn*, 1986). The apparent age of impact melt B is prebasin, so the sample could represent the melt sheet of some large crater that formed on typical highlands terrain in pre-Nectarian time. If it does date a pre-Nectarian impact, it is one of the few such samples that has been analyzed (*Maurer et al.*, 1978; *Ryder*, 1990).

Alternatively, the apparent old age might reflect the presence of clasts that were not degassed during the impact, as *Ryder* (1990) has suggested for other samples with prebasin ^{40}Ar - ^{39}Ar ages. The sample was clast-rich (see Petrography section), and the age was determined by a single extraction, so subtleties in the Ar release pattern would have gone undetected. Thus, we cannot rule out the possibility of undegassed clasts.

Two Luna 20 samples, A and E, have exceptionally young ages, 0.52 Ga and 0.38 Ga, respectively, and therefore must represent crater (rather than basin) impacts. They have the largest Ir/Au ratios of the particles analyzed, 3.7 ± 1.1 and 4.5 ± 0.9 (1σ). Both values are consistent with formation by a chondritic impactor (*Wasson and Kallemeyn*, 1988); the lower ratios in the other samples, approaching unity in B, are more typical of melt rocks produced during basin-forming events (*Anders et al.*, 1973; *Wasson et al.*, 1975). Samples A and E are compositionally distinct and probably represent two separate impacts. Sample A is a relatively coarse-grained impact melt and formed during an impact into an anorthosite-rich terrain. We have no petrographic information about sample E, but macroscopically it also appears to be an impact melt, but one with an unusually low Na_2O concentration (0.18%). Both samples have cosmic-ray exposure ages only slightly shorter than their formation ages, indicating that they were probably ejected from their melt sheets by subsequent impacts soon after their formation.

Impact melt F appears to have some interesting properties. It is compositionally distinct from the local soil at the site, the regional upper crustal composition, and the melt rocks of the Serenitatis or Nectaris Basins (Fig. 6). It is not a unique, or exotic composition, as at least three other Luna 20 rocks (none of them impact melts) are similar to it. It appears to be both more mafic and more KREEP-rich than the typical lunar crust (manifested by the "group 1" composition) and is somewhat analogous in terms of geologic occurrence to the "VHA basalt" composition found at the Apollo 16 site (*Spudis*, 1984), i.e., a "mafic" melt composition found among relatively feldspathic, clastic debris. Melt F has a well-defined age of 3.895 ± 0.017 Ga, an age that places it in the era of major basin formation, perhaps distinct from the ages of the Nectaris (3.92 Ga), Serenitatis (3.87 Ga), and Imbrium (3.85 Ga) Basins, although it falls within the uncertainties of the ages of the samples used to define the Nectaris and Serenitatis events (Fig. 7).

We tentatively associate impact melt F with the Crisium Basin. The Luna 20 site is either inside the topographic basin (*Wilhelms*, 1987) or near its rim crest (*Spudis et al.*, 1989); thus, impact melt from Crisium should constitute at least some of the Luna 20 samples. If particle F is Crisium Basin melt, its more aluminous composition compared with the LKFM or VHA basalt compositions (associated with basins elsewhere on the Moon) could result from the formation of the Crisium Basin in a thicker, more anorthositic crust, farther away from the central nearside of the Moon than Imbrium or Nectaris (*Wilhelms*, 1987). The association of melt F with the Crisium Basin also suggests that Crisium, although younger than Nectaris (*Spudis*, 1984), formed fairly soon afterward, both impacts having occurred around 3.9 Ga.

Although we believe that impact melt F is more likely to be Crisium Basin melt than any other Luna 20 samples so far analyzed, such an identification is by no means certain. As mentioned above, it is also possible that groups 1 or 2 could be Crisium Basin melt, although there are problems with either interpretation (not the least of which is the origin of impact melt F). It is also possible that no Crisium Basin melt has yet been analyzed. In any case, it is clear that Crisium Basin melt is not prominently represented in the Luna 20 collection, so it will be difficult to pin down the age or composition without more sample return missions.

Acknowledgments. This work was supported by NASA grants NAG 9-7 to C. Hohenberg (R.H.N.), NAG 9-56 to L. Haskin (R.L.K.), NAG 9-240 (T.D.S.), NAG 9-454 (G.J.T.), and NGT-50194 (C.T.O.). We are grateful to C. Hohenberg for use of his mass spectrometer and P. Warren for use of unpublished descriptions of particles. R. Strom and M. Magisos assisted in the search through LPL archives for an appropriate photo of the Crisium Basin. Constructive reviews were provided by D. Lindstrom, G. Ryder, and an anonymous reviewer. This is the School of Ocean and Earth Science and Technology Contribution No. 2358 and Planetary Geosciences Division Contribution No. 606.

REFERENCES

- Alexander E. C. Jr. and Davis P. K. (1974) ^{40}Ar - ^{39}Ar ages and trace element contents of Apollo 14 breccias; an interlaboratory cross-calibration of ^{40}Ar - ^{39}Ar standards. *Geochim. Cosmochim. Acta*, **38**, 911-928.
- Anders E., Ganapathy R., Krähenbühl U., and Morgan J. W. (1973) Meteoritic material on the Moon. *Moon*, **8**, 3-24.
- Baldwin R. B. (1987a) On the relative and absolute ages of seven lunar front face basins. I. From viscosity arguments. *Icarus*, **71**, 1-18.
- Baldwin R. B. (1987b) On the relative and absolute ages of seven lunar front face basins. II. From crater counts. *Icarus*, **71**, 19-29.
- Bottomley R. J., York D., and Grieve R. A. F. (1990) ^{40}Ar - ^{39}Ar Argon dating of impact craters. *Proc. Lunar Planet. Sci. Conf. 20th*, pp. 421-431.
- Bower J. F., Wood J. A., Richardson S. M., McSween H. Y. Jr., and Ryder G. (1977) Rock compositions by defocused beam analysis (abstract). In *Abstracts of VIII International Conf. of X-ray Optics and Microanalysis*, p. 182.
- Cadogan P. H. and Turner G. (1977) ^{40}Ar - ^{39}Ar dating of Luna 16 and Luna 20 samples. *Philos. Trans. R. Soc. London*, **A284**, 167-177.
- Davis P. A. and Spudis P. D. (1987) Global petrologic variations on the Moon: A ternary diagram approach. *Proc. Lunar Planet. Sci. 17th*, in *J. Geophys. Res.*, **92**, E387-E395.
- Dence M. R., Grieve R. A. F., and Plant A. G. (1976) Apollo 17 grey breccias and crustal composition in the Serenitatis basin region. *Proc. Lunar Planet. Sci. Conf. 7th*, pp. 1821-1832.
- Deutsch A. and Stöfler D. (1987) Rb-Sr-analyses of Apollo 16 melt rocks and a new age estimate for the Imbrium basin: Lunar basin chronology and the early heavy bombardment of the moon. *Geochim. Cosmochim. Acta*, **51**, 1951-1964.
- Dymek R. E., Albee A. L., and Chodos A. A. (1976) Petrology and origin of Boulders 2 and 3, Apollo 17, Station 2. *Proc. Lunar Sci. Conf. 7th*, pp. 2335-2378.
- Fukuoka T., Laul J. C., Smith M. R., Hughes S. S., and Schmitt R. A. (1986) Chemistry of Yamato-791197 Antarctic meteorite: Evidence for its lunar highlands origin. *Mem. Natl. Inst. Polar Res., Spec. Issue 41*, pp. 84-95. Natl. Inst. of Polar Res., Tokyo.
- Heiken G., Vaniman D., and French B., eds. (1991) *Lunar Sourcebook*. Cambridge Univ., New York, in press.
- Hohenberg C. M. (1980) High-sensitivity pulse-counting mass spectrometer system for noble gas analysis. *Rev. Sci. Instrum.*, **51**, 1075-1082.
- Hohenberg C. M., Marti K., Podosek F. A., Reedy R. D., and Shirck J. R. (1978) Comparisons between observed and predicted cosmogenic noble gases in lunar samples. *Proc. Lunar Planet. Sci. Conf. 9th*, pp. 2311-2344.
- James O. B., Hedenquist J. W., Blanchard D. P., Budahn J. R., and Compston W. (1978) Consortium breccia 73255: Petrology, major- and trace-element chemistry, and Rb-Sr systematics of aphanitic lithologies. *Proc. Lunar Planet. Sci. Conf. 9th*, pp. 789-819.
- Kennedy B. M. (1981) Potassium-argon and iodine-xenon gas retention ages of enstatite chondrite meteorites. Ph.D. thesis, Washington Univ., St. Louis, Missouri. 298 pp.
- Korotev R. L. (1991) Geochemical stratigraphy of two regolith cores from the central highlands of the Moon. *Proc. Lunar Planet. Sci. Conf. 21st*, in press.
- Korotev R. L. and Haskin L. A. (1988) Compositional survey of particles from the Luna 20 regolith (abstract). In *Lunar and Planetary Science XIX*, pp. 635-636. Lunar and Planetary Institute, Houston.
- Laul J. C. and Schmitt R. A. (1973) Chemical composition of Luna 20 rocks and soil and Apollo 16 soils. *Geochim. Cosmochim. Acta*, **37**, 927-942.
- Lindstrom M. M. and Salpas P. A. (1983) Geochemical studies of feldspathic fragmental breccias and the nature of North Ray Crater ejecta. *Proc. Lunar Planet. Sci. Conf. 13th*, in *J. Geophys. Res.*, **87**, A671-A683.
- Lindstrom M. M., Lindstrom D. J., Korotev R. L., and Haskin L. A. (1986) Lunar meteorite Yamato-791197: A polymict anorthositic norite breccia. *Mem. Natl. Inst. Polar Res., Spec. Issue 41*, pp. 58-75. Natl. Inst. of Polar Res., Tokyo.
- Marvin U. B. and Lindstrom M. M. (1983) Rock 67015: A feldspathic fragmental breccia with KREEP-rich melt clasts. *Proc. Lunar Planet. Sci. Conf. 13th*, in *J. Geophys. Res.*, **87**, A659-A670.
- Maurer P., Eberhardt P., Geiss J., Grögler N., Stettler A., Brown G. M., Peckett A., and Krähenbühl U. (1978) Pre-Imbrian craters and basins: Ages, compositions and excavation depths of Apollo 16 breccias. *Geochim. Cosmochim. Acta*, **42**, 1687-1720.
- Ostertag R., Stöfler D., Bischoff A., Palme H., Schultz L., Spettel B., Weber H., Weckwerth G., and Wänke H. (1986) Lunar meteorite Yamato-791197: Petrography, shock history and chemical composition. *Mem. Natl. Inst. Polar Res., Spec. Issue 41*, pp. 17-44. Natl. Inst. of Polar Res., Tokyo.
- Podosek F. A., Huneke J. C., Gancarz A. J., and Wasserburg G. J. (1973) The age and petrography of two Luna 20 fragments and inferences for widespread lunar metamorphism. *Geochim. Cosmochim. Acta*, **37**, 887-904.
- Roddick J. C. (1983) High precision intercalibration of ^{40}Ar - ^{39}Ar standards. *Geochim. Cosmochim. Acta*, **47**, 887-898.
- Ryder G. (1990) Lunar samples, lunar accretion and the early bombardment of the Moon. *Eos Trans. AGU*, **71**, 313, 322-323.
- Ryder G. and Spudis P. D. (1987) Chemical composition and origin of Apollo 15 impact melts. *Proc. Lunar Planet. Sci. Conf. 17th*, in *J. Geophys. Res.*, **92**, E432-E446.
- Simonds C. H. (1975) Thermal regimes in impact melts and the petrology of the Apollo 17 Station 6 boulder. *Proc. Lunar Sci. Conf. 6th*, pp. 641-672.
- Smith M. R., Schmitt R. A., Warren P. H., Taylor G. J., and Keil K. (1983) Far-eastern nonmare samples: New data from Luna 20 and 16 (abstract). In *Lunar and Planetary Science XIV*, p. 716. Lunar and Planetary Institute, Houston.
- Spudis P. D. (1984) Apollo 16 site geology and impact melts: Implications for the geologic history of the lunar highlands. *Proc. Lunar Planet. Sci. Conf. 15th*, in *J. Geophys. Res.*, **89**, C95-C107.

- Spudis P.D. and Ryder G. (1981) Apollo 17 impact melts and their relation to the Serenitatis basin. In *Multi-ring Basins, Proc. Lunar Planet. Sci. 12A* (P.H. Schultz and R. B. Merrill, eds.), pp. 133-148. Pergamon, New York.
- Spudis P.D., Hawke B. R., and Lucey P. G. (1989) The lunar Crisium basin: Geology, rings, and deposits (abstract). In *Lunar and Planetary Science XXI*, pp. 1042-1043. Lunar and Planetary Institute, Houston.
- Steiger R. H. and Jäger E. (1977) Subcommittee of geochronology: Convention on the use of decay constants in geo- and cosmochemistry. *Earth Planet. Sci. Lett.*, *36*, 359-362.
- Swindle T., Spudis P. D., Taylor G. J., Korotev R., Nichols R. H., and Olinger C. T. (1990) Searching for Crisium basin ejecta: Chemistry and ages of Luna 20 impact melts (abstract). In *Lunar and Planetary Science XXI*, pp. 1229-1230. Lunar and Planetary Institute, Houston.
- Turner G., Huneke J. C., Podosek F. A., and Wasserburg G. J. (1971) ^{40}Ar - ^{39}Ar ages and cosmic ray exposure ages of Apollo 14 samples. *Earth Planet. Sci. Lett.*, *12*, 19-35.
- Turner G., Huneke J. C., Podosek F. A., and Wasserburg G. J. (1972) Ar^{40} - Ar^{39} systematics in rocks and separated minerals from Apollo 14. *Proc. Lunar Sci. Conf. 3rd*, pp. 1589-1612.
- Turner G., Enright M. C., and Cadogan P. H. (1978) The early history of chondrite parent bodies inferred from ^{40}Ar - ^{39}Ar ages. *Proc. Lunar Planet. Sci. Conf. 9th*, pp. 989-1025.
- Warner J. L., Simonds C. H., and Phinney W. C. (1976) Apollo 17, Station 6 boulder sample 76255: Absolute petrology of breccia matrix and igneous clasts. *Proc. Lunar Sci. Conf. 7th*, pp. 2233-2250.
- Warren P. H. and Kallemeyn G. W. (1986) Geochemistry of lunar meteorite Yamato-791197: Comparison with ALHA81005 and other lunar samples. *Mem. Natl. Inst. Polar Res., Spec. Issue 41*, pp. 3-16. Natl. Inst. of Polar Res., Tokyo.
- Wasson J. T. and Kallemeyn G. W. (1988) Composition of chondrites. *Philos. Trans. R. Soc. London*, *A325*, 535-544.
- Wasson J. T., Boynton W. V., and Chou C.-L. (1975) Compositional evidence regarding the influx of interplanetary materials onto the lunar surface. *Moon*, *13*, 121-141.
- Wilhelms D. E. (1987) *The Geologic History of the Moon*. U.S. Geol. Surv. Prof. Pap. 1348. 302 pp.
- Winzer S. R., Nava D. F., Schuhmann P. J., Lum R. K. L., Schuhmann S., Lindstrom M. M., Lindstrom D. J., and Philpotts J. A. (1977) The Apollo 17 "melt sheet": Chemistry, age and Rb/Sr systematics. *Earth Planet. Sci. Lett.*, *33*, 389-400.
- Wolfe E. W., Bailey N. G., Lucchitta B. K., Muehlberger W. R., Scott D. H., Sutton R. L., and Wilshire H. G. (1981) *The Geologic Investigation of the Taurus-Littrow Valley: Apollo 17 Landing Site*. U.S. Geol. Surv. Prof. Pap. 1080. 280 pp.
- Wood J. A. (1975) The nature and origin of boulder 1, station 2, Apollo 17. *Moon*, *14*, 505-517.
- Yaniv A. and Heymann D. (1972) Atmospheric Ar^{40} in lunar fines. *Proc. Lunar Sci. Conf. 3rd*, pp. 1967-1980.